Check for updates

Annals of the New York Academy of Sciences

ANNALS OF THE NEW YORK ACADEMY OF SCIENCES

ORIGINAL ARTICLE

Male Reproductive and Cellular Damage After Prenatal 3.5 GHz Radiation Exposure: One-Year Postnatal Effects

Elif Gelenli Dolanbay[1] | Tugay Mert[1] | Gozde Caliskan Bender[1] | Hava Bektas[2] | Unal Uslu[1] | Claudio Enrique Fernandez-Rodriguez[3] | Suleyman Dasdag[4]

[1]Department of Histology and Embryology, Faculty of Medicine, Istanbul Medeniyet University, Istanbul, Turkey | [2]Department of Biophysics, Faculty of Medicine, Van Yuzuncu Yıl University, Van, Turkey | [3]Rio Grande do Sul Federal Institute of Education, Science and Technology, Bento Gonçalves, Brazil | [4]Department of Biophysics, Faculty of Medicine, Istanbul Medeniyet University, Istanbul, Turkey

Correspondence: Elif Gelenli Dolanbay (elif.dolanbay@medeniyet.edu.tr)

Received: 2 June 2025 | **Revised:** 7 August 2025 | **Accepted:** 16 September 2025

Keywords: 3.5 GHz RFR | autophagy | DNA damage | prenatal exposure | sperm morphology | testis

Abstract

This study investigates the long-term effects of prenatal exposure to 3.5 GHz radiofrequency radiation (RFR) on male reproductive health. Pregnant Wistar Hannover rats were divided into sham control, full-gestation exposure (3T RFR), and late-gestation exposure (2T RFR) groups (2 h/day). Male offspring were euthanized at 12 months for testicular analysis. In the 3T RFR group, seminiferous tubule diameter and epithelial height were significantly reduced compared to controls (adjusted $p = 0.03$ and 9.71×10^{-8}), along with lower Johnsen scores (adjusted $p = 0.022$). Abnormal sperm morphology increased significantly (adjusted $p = 0.036$). γ-H2AX immunostaining scores were elevated in the 2T and 3T groups (adjusted $p = 0.012$ and 6.36×10^{-9}). Beclin-1 expression was significantly higher in the 3T group versus sham and 2T groups (adjusted $p = 8.55 \times 10^{-4}$ and 4.51×10^{-6}). TUNEL-positive cell counts were significantly higher in both RFR groups than in sham (adjusted $p = 8.77 \times 10^{-18}$ for 3T, 6.42×10^{-17} for 2T), as was the apoptosis index (adjusted $p = 8.77 \times 10^{-18}$ for 3T, 5.66×10^{-17} for 2T). All p values were Holm–Bonferroni corrected. These findings indicate that prenatal exposure to 3.5 GHz RFR results in persistent testicular damage, impaired spermatogenesis, and increased DNA damage, autophagy, and apoptosis in adult male rats.

1 | Introduction

Radiofrequency radiation (RFR) is a type of nonionizing radiation that occupies the low-energy end of the electromagnetic spectrum, ranging from 30 kHz to 300 GHz [1]. This form of radiation is widely utilized in modern telecommunications, including television and radio transmission, cellular networks, microwave ovens, and Wi-Fi technologies [2]. Given its extensive applications in daily life, RFR has become an integral part of modern society. However, the increasing reliance on RFR-emitting devices has raised concerns regarding their potential health effects, particularly their impact on sensitive biological systems.

In the past decade, advancements in wireless communication technologies have significantly enhanced connectivity, providing faster data transmission and greater bandwidth across various sectors, such as commerce, education, healthcare, and consumer applications. While these technological advancements offer numerous benefits, they have also raised health concerns. Previous reports have linked RFR exposure to headaches, sleep disorders [3], male infertility [4], and, more controversially, an increased risk of cancer [5, 6]. Among these concerns, the potential impact of RFR on male reproductive health has gained attention, particularly due to the proximity of devices like cell phones to sensitive reproductive organs [1, 7, 8]. Exposure to 3.5 GHz RFR, a frequency widely used in emerging 5G

© 2025 The New York Academy of Sciences.

technologies, has specifically raised concerns due to its unique energy absorption characteristics and potential to penetrate biological tissues, including the male reproductive system [9].

Some previous studies indicated associations between RFR exposure and reduced sperm quality, decreased motility, and increased oxidative stress in testicular tissues [8, 10, 11]. The BioInitiative Report (2012) highlighted that RFR exposure can trigger epigenetic changes, interfere with DNA repair mechanisms, and induce de novo mutations, which may lead to reproductive failure, including sperm damage and increased miscarriage risk [12]. However, some other studies on the subject provided contrary results, as they reported negligible effects of RFRs on the testes [13–16]. Intrauterine RFR exposure is a critical subject of investigation due to the radiation sensitivity of the developing organs [2].

In addition to male fertility, RFR exposure during pregnancy has raised concerns regarding fetal development. Changes in maternal physiology induced by radiation may directly or indirectly affect the fetus in the form of an increased risk of congenital anomalies, developmental disorders, and childhood cancer [17–20]. Nevertheless, some other researchers have found no significant association between fetal development and RFR exposure [21]. Such discrepancies may arise from differences in study methodologies, exposure durations, or variations in the developmental stages during which the exposure occurred. These inconsistencies highlight the need for further research to elucidate the potential risks of RFR exposure during critical developmental periods.

H2AX is a unique histone due to its ability to undergo phosphorylation at the serine 139 residue upon DNA damage, forming γ-H2AX, and thus plays a vital role in the DNA repair processes. This phosphorylated form serves as a sensitive biomarker of DNA double-strand breaks (DSBs), which are critical indicators of genomic instability and cellular stress [22, 23]. Radiation-induced DSBs lead to the accumulation of γ-H2AX foci, enabling precise detection of DNA damage caused by RFR [24].

Autophagy is an important mechanism in which the unnecessary cellular materials and parts are removed in lysosomes. This mechanism is essential for maintaining cellular homeostasis and is activated by stressors such as hypoxia, oxidative stress, and nutrient deprivation [25, 26]. Research suggests that RFR can influence autophagy, predominantly through nonthermal mechanisms such as oxidative stress [27–30]. Beclin-1, a critical regulator of autophagy, interacts with various cofactors to promote autophagic activity, underscoring its central role in cellular stress responses [31].

Apoptosis is the mechanism of controlled death of the cell, which plays significant roles in maintaining tissue homeostasis in various processes such as the regulation of the immune system and embryogenesis. Several chemical or physical changes, such as radiation or oxidative stress, can signal the beginning of apoptosis [32]. The apoptotic process is known to be started by two main pathways: intrinsic and extrinsic. The intrinsic pathway can be triggered by irradiation, oxidative stress, or varioustoxic chemicals. The activation of these pathways leads to processes involving intracellular caspases and ultimately to DNA degradation. The sign of apoptosis is the endonuclease-catalyzed degradation of DNA [33]. The TUNEL assay, a widely used technique to detect DNA fragmentation during apoptosis, enables precise visualization of apoptotic activity in situ [32].

Despite the accumulated knowledge regarding RFR's effects, the long-term consequences of prenatal RFR exposure on male reproductive health remain underexplored. Their widespread usage makes understanding their potential impact on molecular pathways crucial. Thus, the purpose of this study is to investigate whether the reproductive systems of male rats exposed to 3.5 GHz RFRs exclusively in the prenatal period were affected in the first year after birth.

2 | Materials and Methods

2.1 | Animal Experimentation and Groups

The study was performed on 18 adult male Wistar Hannover rats (12 months old and weighing 350–400 g) with and without intrauterine RFR exposure. To minimize potential confounding factors, all animals were handled by trained personnel in a consistent manner. The animal testing phase of this experimental study was conducted in the Experimental Animal Research and Application Laboratory of the Bağcılar Training and Research Hospital, University of Health Sciences. All stages of the study were designed and carried out according to the guidelines of the institution's Local Ethics Committee for Animal Experiments (Protocol No: 2024-16).

The study was designed to include three groups, one sham control and two experimental (3.5 GHz RFR exposure). Considering the approximately 21-day gestational period in rats, each week is often referred to as a trimester to provide a comparative framework with human pregnancy. The first experimental group is exposed to RFR throughout the pregnancy (three trimesters RFR), and the second experimental group is exposed to RFR in the last 2 weeks of pregnancy (two trimesters RFR). In both experimental groups, exposure was limited to 2 h/day. External radiation was avoided by keeping the animals in Faraday cages during experimental exposure. After birth, 18 male offspring with birth weights ranging from 5 to 7 g were randomly assigned to the sham control and two experimental RFR exposure groups, with six animals in each group, and followed for 12 months. These criteria ensured consistency across groups while fully preserving the integrity of the randomization and blinding procedures. Rats were fed ad libitum with water and feed (rat chow) under conventional conditions and kept at 24 ± 1°C ambient temperature, 12 h light/12 h dark. At the end of 12 months, rats in all groups were euthanized with high doses of anesthetic, and animals were sacrificed by cardiac blood puncture. Testes and epididymis tissues were removed for examination. For histologic and immunohistochemical examination, the testes were fixed in Bouin's fixative.

2.2 | Exposure and Field Measurements

A GSM signal generator (model 3500 PM10, Everest Comp., Adapazarı, Turkey), which generates a radiofrequency waveform

17496632, 0, Downloaded from https://nyaspubs.onlinelibrary.wiley.com/doi/10.1111/nyas.70116 by Univ of California Lawrence Berkeley National Lab, Wiley Online Library on [11/11/2025]. See the Terms and Conditions (https://onlinelibrary.wiley.com/terms-and-conditions) on Wiley Online Library for rules of use; OA articles are governed by the applicable Creative Commons License

modulated in the 3.5 GHz GSM band, was utilized to expose rats to RFR resembling the frequency to that generated by mobile phones. The power output of the signal generator was kept at 1 W during the exposure period. The piece of the generator that functions as the antenna was designed to replicate that of a conventional mobile phone.

The Plexiglas cages in which the rats were irradiated were the same size as standard animal feeding cages and were designed specifically for this study (the lids were also made of Plexiglas, inspired by standard cages). These specially designed cages contained no metal parts. Even the tip of the water bottle used by the animals was made of Plexiglas tubing, specifically for this study. The cages were designed to ensure optimal RFR radiation exposure. Pregnant rats in the experimental groups were exposed to 3.5 GHz RFRs for 2 h/day, only during pregnancy, allowing them to roam freely within these cages. Animals in the sham control group were also kept in the same experimental circumstances but the signal generator turned off. To protect animals from environmental factors such as RFR, and so forth, each group in the cages was housed in the separate Faraday cages throughout the irradiation. The signal generator was located outside the Faraday cage, but its antenna was located inside the cage, 50 cm above the animals. The antenna was positioned directly in the center of the cage. A metal reflector was placed above the antenna.

After birth, male pups were separated and not exposed to any RFR until the pups were 12 months old, meaning they were 1-year old. Thus, the offspring were exposed to 3.5 GHz RFRs only while in utero. In this way, the male reproductive and cellular damage status of the rats exposed to these RFRs only while in utero was monitored 1 year later.

EMR 300 (NARDA, Pfullingen, Germany) was used to measure the electric fields. E field measurements were performed with an EMR 300 in the corners and at the center of the cages we used in our study, which are the same size as standard animal cages. E fields were measured as 24 V/m, 26 V/m, 26.3 V/m, and 27 V/m at the corners, while 28 V/m was measured at the center of the cage.

2.3 | Specific Absorption Rate Analysis

CST Studio software (CST AG, Darmstadt, Germany) was used to simulate specific absorption rate (SAR) at the rat's uterus. The technical setup used in the simulation was meticulously designed to closely mirror the actual experimental configuration. The 3D electromagnetic field (EMF) solver CST (CST AG, Darmstadt, Germany) was employed to model the applicator antenna along with its reflector, the Plexiglas carousel, and the rat. A highly detailed rat model, based on computerized tomography (CT) scans, is provided within CST's biological models library. This voxel-based model is comprehensive and includes all the tissues found in a rat.

The CST software employs the finite integration technique (FIT), a method that involves both differential and integral solvers to operate simultaneously, enabling accurate electromagnetic and thermal simulations. To validate the simulation's accuracy, the electric field values generated were compared with those measured experimentally using the EMR 300 field probe (NARDA, Pfullingen, Germany). The electric field strength generated by the EMF generator was measured at five distinct points on the exposure plane where the animals were located: the four corners and the center. Measurements were conducted using a calibrated EMR-300 device (Narda Safety Test Solutions, Germany). No significant variation was observed among the measured values, which ranged between 24 and 27 V/m. The average field strength at the center was determined to be 28 V/m. These results indicate that the EMF was uniformly distributed across the exposure plane. Considering the homogeneity of the field, peak spatial SAR (psSAR) simulations were performed based on this average electric field strength using CST Studio Suite software, with the frequency set to 3.5 GHz.

Furthermore, the exposure plane was kept fixed throughout the experiment, and care was taken to avoid the presence of any metallic surfaces that could cause electromagnetic reflection. psSAR calculations accounted for the thermal effects of EMF exposure. However, no observable changes in body temperature were detected during the exposure period.

2.4 | Sperm Analysis

Following the creation of incisions on the cauda of both epididymis tissues with a scalpel, semen was collected into Eppendorf tubes containing 1 mL of Ringer lactate and mixed. After 10 μL of the supernatant was spread on a slide, it was allowed to dry, fixed with 96% ethanol, stained using the Giemsa method, and sperm morphology was evaluated. The slides were subjected to a detailed evaluation of sperm morphology by scoring 1000 spermatozoa per animal. The spermatozoa were categorized as normal or abnormal. Abnormal spermatozoa were defined as spermatozoa exhibiting head abnormalities and/or tail abnormalities [34].

2.5 | Histological and Immunohistochemical Studies

Bouin-fixed testicular tissues underwent tissue processing, embedded as paraffin blocks, and 5 μm sections underwent hematoxylin and eosin (H&E) staining for histologic evaluation. Histologic evaluation was performed with light microscopy (Olympus BX53) in 20 randomly selected seminiferous tubules according to Johnsen scoring, and tubule diameters with seminiferous epithelium height were measured [35].

Five-micrometer sections were examined immunohistochemically using γ-H2AX and Beclin-1 primary antibodies to assess DNA damage, apoptosis, and autophagy. After the deparaffinization of the sections in xylene, they were rehydrated in alcohol series with decreasing alcohol content, and then endogenous peroxidases were inactivated by incubation with Ultravision Hydrogen Peroxide Block. Sections were treated with Ultrablock to prevent nonspecific background staining. Sections were incubated overnight at 4°C with primary antibodies for Beclin-1 (1:200 dilutions, cat. no. AC-0276RUO, Epitomics Burlingame, CA, USA) and γ-H2AX antibody (1:400 dilutions, cat. no. ab81299, Abcam, Cambridge, UK). A

17496632, 0, Downloaded from https://nyaspubs.onlinelibrary.wiley.com/doi/10.1111/nyas.70116 by Univ of California Lawrence Berkeley National Lab, Wiley Online Library on [11/11/2025]. See the Terms and Conditions (https://onlinelibrary.wiley.com/terms-and-conditions) on Wiley Online Library for rules of use; OA articles are governed by the applicable Creative Commons License

secondary antibody and streptavidin-biotin-peroxidase complex (Ultravision Detection System, cat. no. TP-125-HL, Thermo Fisher Scientific, Waltham, MA, USA) were then applied for 10 min, and color development was achieved using diaminobenzidine (DAB). The preparations were examined by light microscopy (Olympus BX53). The scoring of the staining was done as 0 (no staining), 1 (weak staining), 2 (moderate staining), and 3 (strong staining). For immunohistochemical evaluation, a random selection of 10 stained seminiferous tubules were performed for each animal, and the H-score was calculated semiquantitatively using the positive staining intensity and percentage [36].

The In Situ Cell Death Detection Kit POD (cat. No. 11684817910; Roche Diagnostics, Mannheim, Germany) was used for the TUNEL study, and the protocol was performed as described by the manufacturer. Deparaffinized and rehydrated 5 µm sections were taken from paraffin blocks on positively charged slides. Endogenous peroxidase activity was suppressed with hydrogen peroxide in the tissue permeabilized with proteinase K at 37°C for 15 min. In the TUNEL reaction mixture prepared with 50 µL of enzyme solution and 450 µL of label solution, the slides were incubated in an oven at 37°C for 1 h. To examine the reaction product under the light microscope, the color formation was achieved by using DAB chromogen after incubation with converter solution at 37°C for 30 min. The slides were counterstained with hematoxylin and coverslipped with a synthetic mounting medium. For apoptotic index measurement, the ratio of positively stained cells to all cells in ten randomly selected areas on each slide was calculated [37].

Histological and immunohistochemical evaluation was performed by investigators blinded to the experimental groups to ensure unbiased assessment.

2.6 | Statistical Analysis

Statistical Package for Social Sciences (SPSS; for Windows; version 18.0; SPSS Inc. Chicago, IL, USA) package program was used for the statistical analysis of the obtained data. The data distribution was evaluated using the Shapiro–Wilk test. The variations between the groups in terms of γ-H2AX, Beclin-1, STD, and JS were assessed with the Kruskal–Wallis test. Post hoc 97 multiple comparison test was performed to determine which group or groups the difference originated from. Differences between the groups in terms of SEH, sperm morphology, TUNEL, and apoptosis index were analyzed by ANOVA test, and the Duncan test was utilized to determine the origin of the difference. To control for the risk of Type I error from multiple comparisons, the Holm–Bonferroni correction was applied to the p values of all pairwise post hoc tests. The significant p values were denoted as $p < 0.05$ (*), $p < 0.01$ (**), and $p < 0.001$ (***) [38]. All data were reported as the mean and ± standard error of the mean.

3 | Results

3.1 | SAR Results

The SAR calculations were conducted using the IEEE/IEC 62704-1 standard to assess the distribution of SAR values. The psSAR for 1 g was 0.06622 mW/g, and for 10 g was 0.03825 mW/g.

3.2 | Histological Evaluation of the Testes

Histopathological evaluation with H&E staining revealed preserved testicular architecture in the sham control group, while the RFR-exposed groups exhibited varying degrees of seminiferous tubule degeneration and germ cell loss (Figure 1).

The mean Johnsen score was 9.34 ± 0.08 in the sham control group, 8.84 ± 0.08 in the 2T RFR group, and 9.04 ± 0.08 in the 3T RFR group. Statistically significant differences were found between the sham control and 2T RFR groups (adjusted $p = 4.56 \times 10^{-4}$), and between the sham control and 3T RFR groups (adjusted $p = 0.022$). The difference between the 2T and 3T RFR groups was not statistically significant (adjusted $p = 0.792$).

The diameter of the seminiferous tubule was measured at 308.44 ± 4.51 µm in the sham control group, 314.33 ± 3.78 µm in the 2T RFR group, and 287.90 ± 6.08 µm in the 3T RFR group. A statistically significant decrease was observed in the 3T RFR group compared to both the sham control (adjusted $p = 0.03$) and 2T RFR groups (adjusted $p = 0.0022$). The difference between the sham control and 2T RFR groups was not statistically significant (adjusted $p = 1.000$).

The SEH was measured as 87.33 ± 1.72 µm in the sham control group, 83.34 ± 1.46 µm in the 2T RFR group, and 70.05 ± 1.60 µm in the 3T RFR group. Statistically significant reductions were found in the 3T RFR group compared to both the sham control (adjusted $p = 9.71 \times 10^{-8}$) and 2T RFR groups (adjusted $p = 5.01 \times 10^{-7}$). The difference between the sham control and 2T RFR group was not significant (adjusted $p = 1.000$).

As illustrated in Figure 1, a bar graph is employed to summarize the comparative data and significance levels for all histological evaluations.

3.3 | Epididymal Sperm Morphology Results

The observed morphological abnormalities in rat sperm included aberrations such as double tails, detached heads, detached tails, coiled tails, bent midpieces, and irregularly shaped heads (Figure 2).

The percentage of morphologically abnormal spermatozoa was 26.26 ± 2.16% in the sham control group, 36.18 ± 3.54% in the 2T RFR group, and 40.48 ± 3.57% in the 3T RFR group. A statistically significant increase was observed in the 3T RFR group compared with the sham control (adjusted $p = 0.036$). However, the differences between the sham control and 2T RFR groups (adjusted $p = 0.882$), as well as between the 2T and 3T RFR groups (adjusted $p = 0.616$), were not statistically significant after Holm–Bonferroni correction (Figure 2).

3.4 | Immunohistochemistry Results

3.4.1 | γ-H2AX Immunostaining

Immunohistochemical analysis revealed increased γ-H2AX expression, particularly in the 3T RFR group, consistent with

17496632, 0, Downloaded from https://nyaspubs.onlinelibrary.wiley.com/doi/10.1111/nyas.70116 by Univ of California Lawrence Berkeley National Lab, Wiley Online Library on [11/11/2025]. See the Terms and Conditions (https://onlinelibrary.wiley.com/terms-and-conditions) on Wiley Online Library for rules of use; OA articles are governed by the applicable Creative Commons License

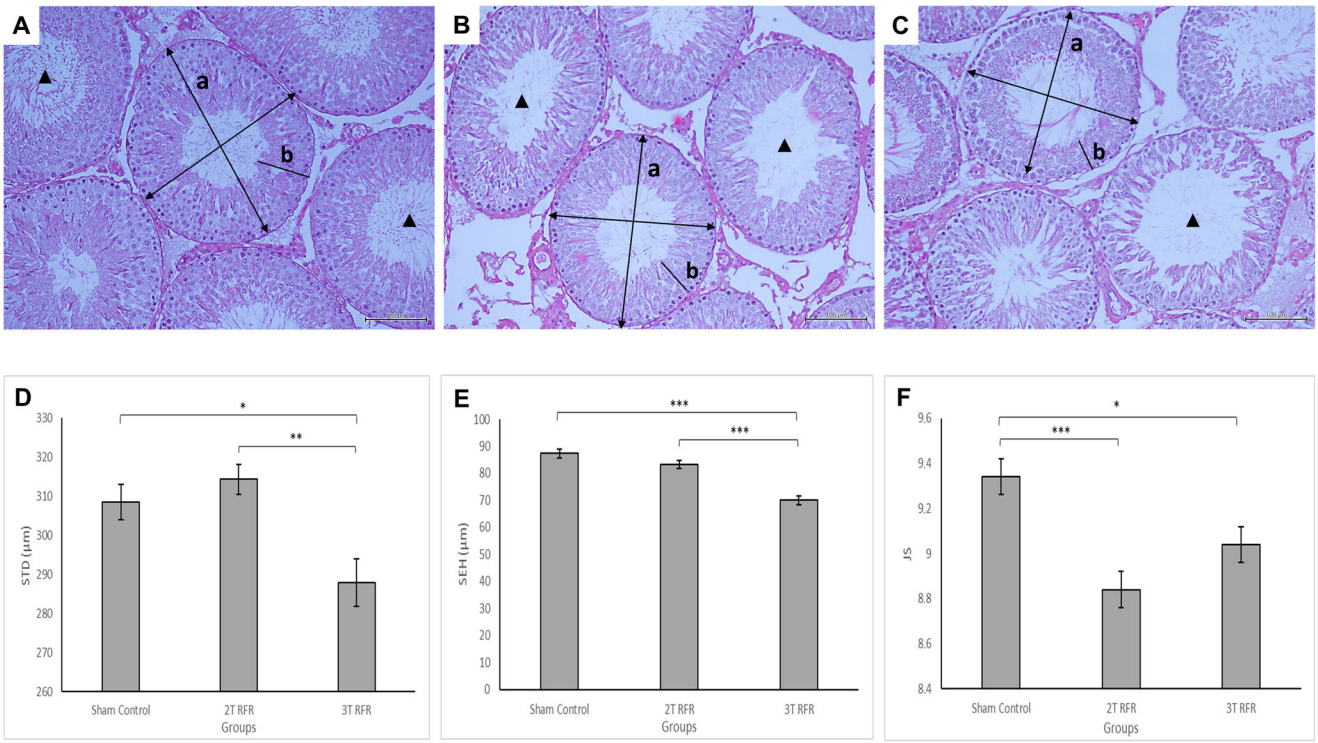


FIGURE 1 | Hematoxylin and eosin (H&E) staining and histomorphometric analysis of testicular tissue. Panels A–C show representative H&E-stained sections from the sham control (A), 2T RFR (B), and 3T RFR (C) groups. Arrowheads indicate spermatogenic cells that have progressed to the spermatozoa stage. Panels D–F present bar graphs showing the mean seminiferous tubule diameter (D), seminiferous epithelium height (E), and Johnsen score (F) in the sham control, 2T RFR, and 3T RFR groups. Compared to the sham control group, both seminiferous tubule diameter (STD) and epithelial height (SEH) decreased after RFR exposure; the most pronounced decreases were observed in the 3T group. Similarly, the Johnsen score (JS) also decreased in the 3T RFR group. Data are presented as mean ± SE. Statistical significance: $p < 0.05$ (*), $p < 0.01$ (**), $p < 0.001$ (***), based on Holm–Bonferroni corrected p values (H&E staining; scale bar = 100 μm).

elevated DNA damage levels. Representative micrographs demonstrating the distribution and intensity of γ-H2AX immunoreactivity across the experimental groups are presented in Figure 3.

The γ-H2AX immunostaining H-score was lowest in the sham control group (135.00 ± 9.10), increased in the 2T RFR group (175.50 ± 5.64), and was highest in the 3T RFR group (204.75 ± 4.08). Statistically significant differences were found between the sham control and 2T RFR groups (adjusted $p = 0.012$), the sham control and 3T RFR groups (adjusted $p = 6.36 \times 10^{-9}$), and between the 2T and 3T RFR groups (adjusted $p = 0.0021$).

3.4.2 | Beclin-1 Immunostaining

Beclin-1 immunostaining showed weak cytoplasmic expression in the sham group, with notably increased staining intensity in germ cells of the RFR-exposed groups, suggesting enhanced autophagic activity (Figure 4).

The results showed that the Beclin-1 immunostaining H-scores were 167.90 ± 4.56 in the sham control group, 162.42 ± 4.18 in the 2T RFR group, and 194.25 ± 3.45 in the 3T RFR group. The 3T RFR group exhibited significantly higher expression compared to both the sham control (adjusted $p = 8.55 \times 10^{-4}$) and 2T RFR groups (adjusted $p = 4.51 \times 10^{-6}$). The difference between the sham control and 2T RFR group was not statistically significant (adjusted $p = 1.000$).

3.5 | TUNEL Assay Results

The TUNEL assay revealed a low number of apoptotic cells in the sham control testes, whereas a significant increase in TUNEL-positive nuclei was observed in the 2T and 3T RFR groups (Figure 5).

The number of TUNEL-positive cells was 5.18 ± 0.70 in the sham control group, 67.10 ± 6.18 in the 2T RFR group, and 70.33 ± 5.34 in the 3T RFR group. Both RFR groups showed significantly higher numbers compared to the sham control (adjusted $p = 6.42 \times 10^{-17}$ for 2T; adjusted $p = 8.77 \times 10^{-18}$ for 3T). The difference between the 2T and 3T RFR groups was not significant (adjusted $p = 1.000$).

The apoptosis index was determined to be 3.80 ± 0.70 in the sham control group, 37.96 ± 8.17 in the 2T RFR group, and 38.92 ± 5.79 in the 3T RFR group. Both experimental groups showed significantly increased indices compared to the sham control (adjusted $p = 5.66 \times 10^{-17}$ for 2T; adjusted $p = 7.17 \times 10^{-18}$ for 3T). No significant difference was found between the 2T and 3T RFR groups (adjusted $p = 1.000$).

17496632, 0, Downloaded from https://nyaspubs.onlinelibrary.wiley.com/doi/10.1111/nyas.70116 by Univ of California Lawrence Berkeley National Lab, Wiley Online Library on [11/11/2025]. See the Terms and Conditions (https://onlinelibrary.wiley.com/terms-and-conditions) on Wiley Online Library for rules of use; OA articles are governed by the applicable Creative Commons License

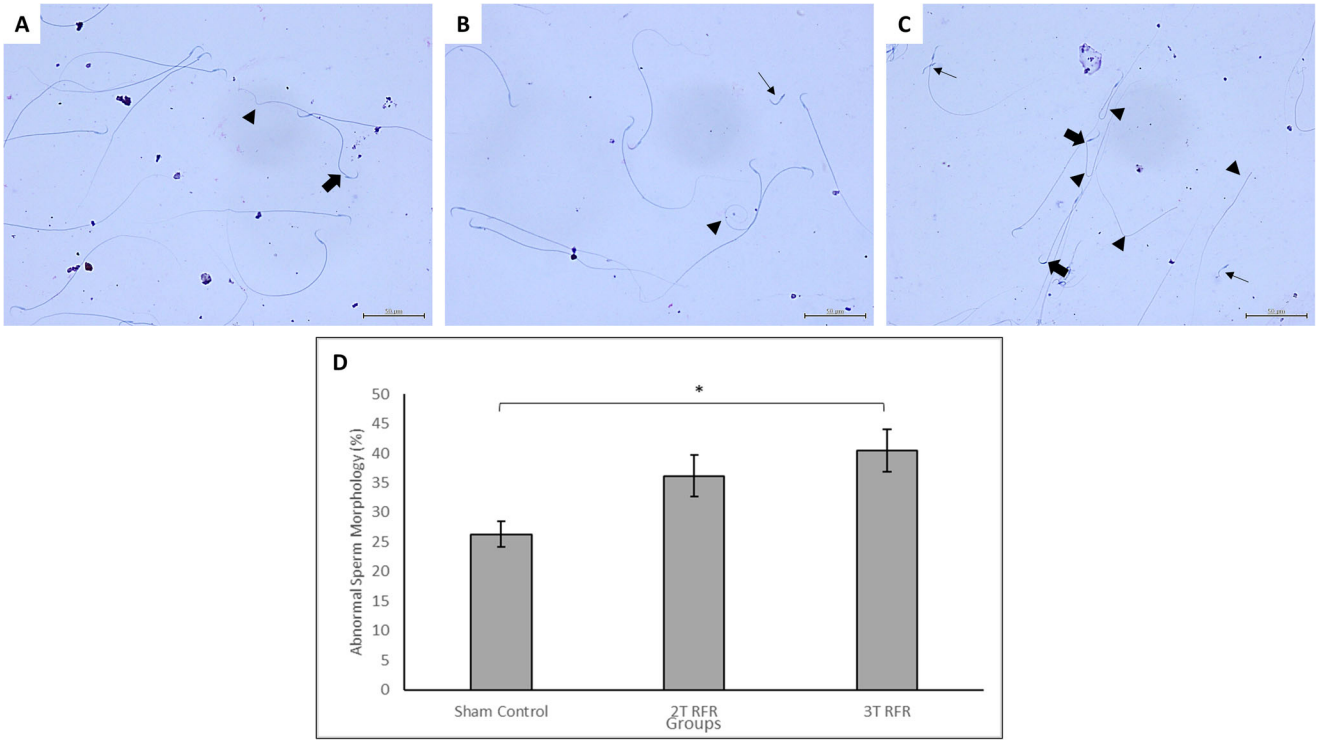


FIGURE 2 | Sperm morphology results. Panels A–C show representative microscopic images of spermatozoa from the sham control (A), 2T RFR (B), and 3T RFR (C) groups. Thin arrows indicate head abnormalities, thick arrows indicate neck abnormalities, and arrowheads indicate tail abnormalities. Panel D presents a bar graph showing the frequency of morphological abnormalities in each group. RFR exposure increased the frequency of sperm defects, particularly in the 3T RFR group. Data are presented as mean ± SE. Statistical significance: $p < 0.05$ (*), $p < 0.01$ (**), $p < 0.001$ (***), based on Holm–Bonferroni corrected p values (Giemsa staining; scale bar = 50 μm).

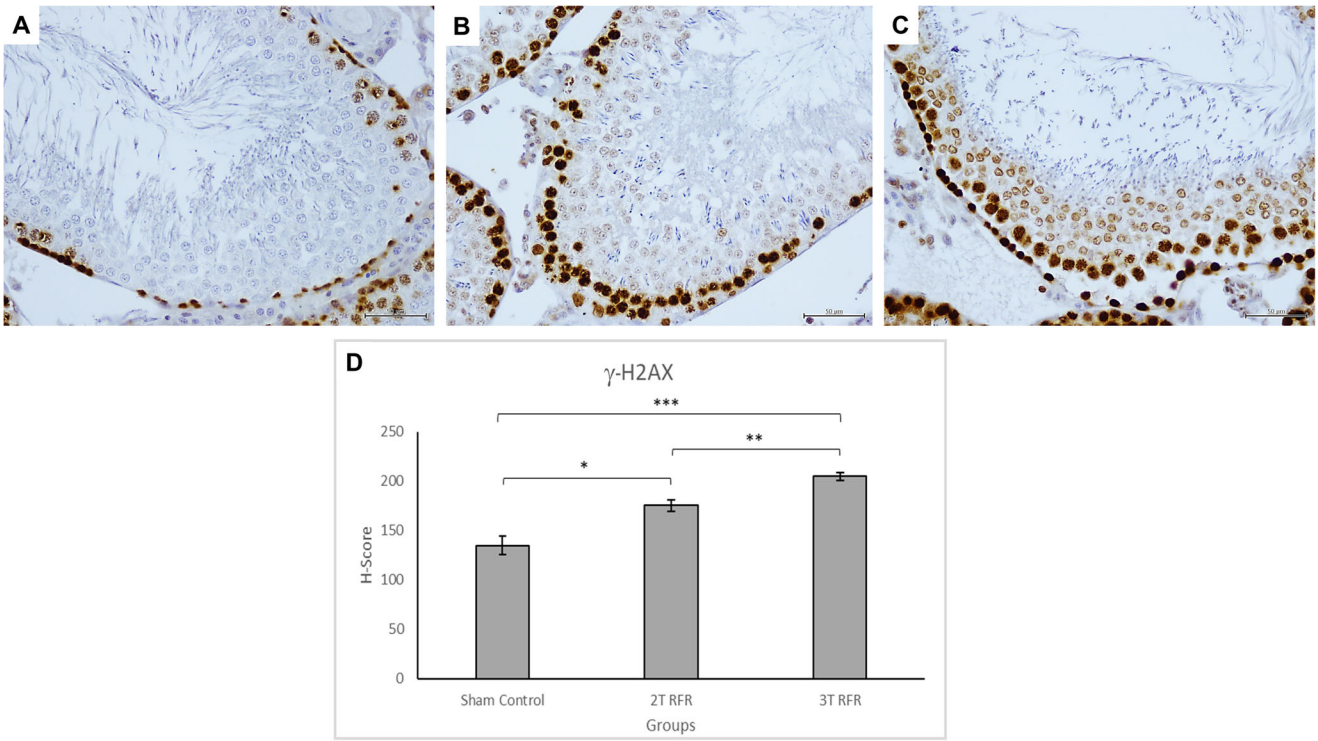


FIGURE 3 | γ-H2AX immunohistochemical staining. Panels A–C show representative γ-H2AX-stained sections from the sham control (A), 2T RFR (B), and 3T RFR (C) groups. Panel D shows the quantitative expression of γ-H2AX as the H-score. The intensity of γ-H2AX nuclear staining increases with prolonged exposure to RFR, being most prominent in the 3T RFR group. Data are presented as mean ± SE. Statistical significance: $p < 0.05$ (*), $p < 0.01$ (**), $p < 0.001$ (***), based on Holm–Bonferroni corrected p values. The scale bar is 50 μm.

17496632, 0, Downloaded from https://nyaspubs.onlinelibrary.wiley.com/doi/10.1111/nyas.70116 by Univ of California Lawrence Berkeley National Lab, Wiley Online Library on [11/11/2025]. See the Terms and Conditions (https://onlinelibrary.wiley.com/terms-and-conditions) on Wiley Online Library for rules of use; OA articles are governed by the applicable Creative Commons License

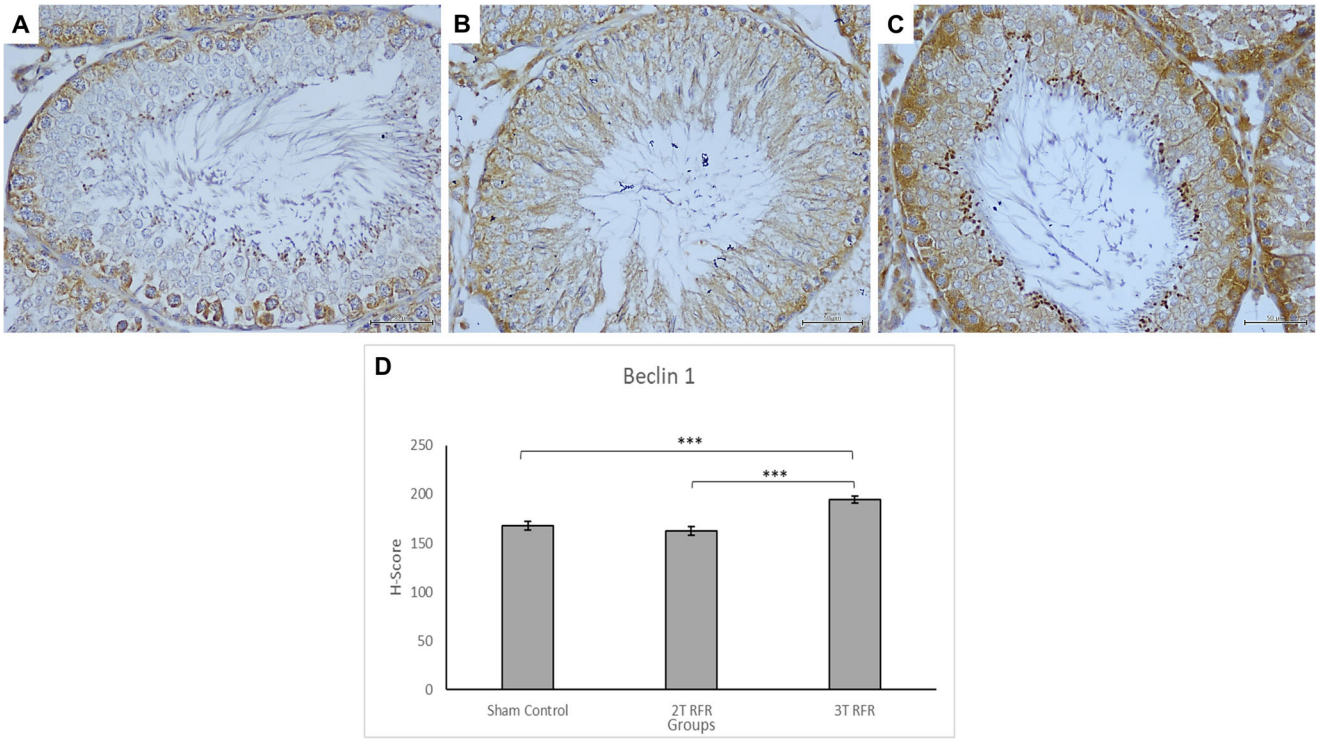


FIGURE 4 | Beclin-1 immunohistochemical staining. Panels A–C show representative Beclin-1-stained sections from the sham control (A), 2T RFR (B), and 3T RFR (C) groups. Panel D shows the quantitative expression of Beclin-1 as the H-score. The cytoplasmic staining becomes more pronounced with extended exposure to radiofrequency radiation, showing the highest levels in the 3T RFR group. Data are presented as mean ± SE. Statistical significance: $p < 0.05$ (*), $p < 0.01$ (**), $p < 0.001$ (***), based on Holm–Bonferroni corrected p values. The scale bar is 50 μm.

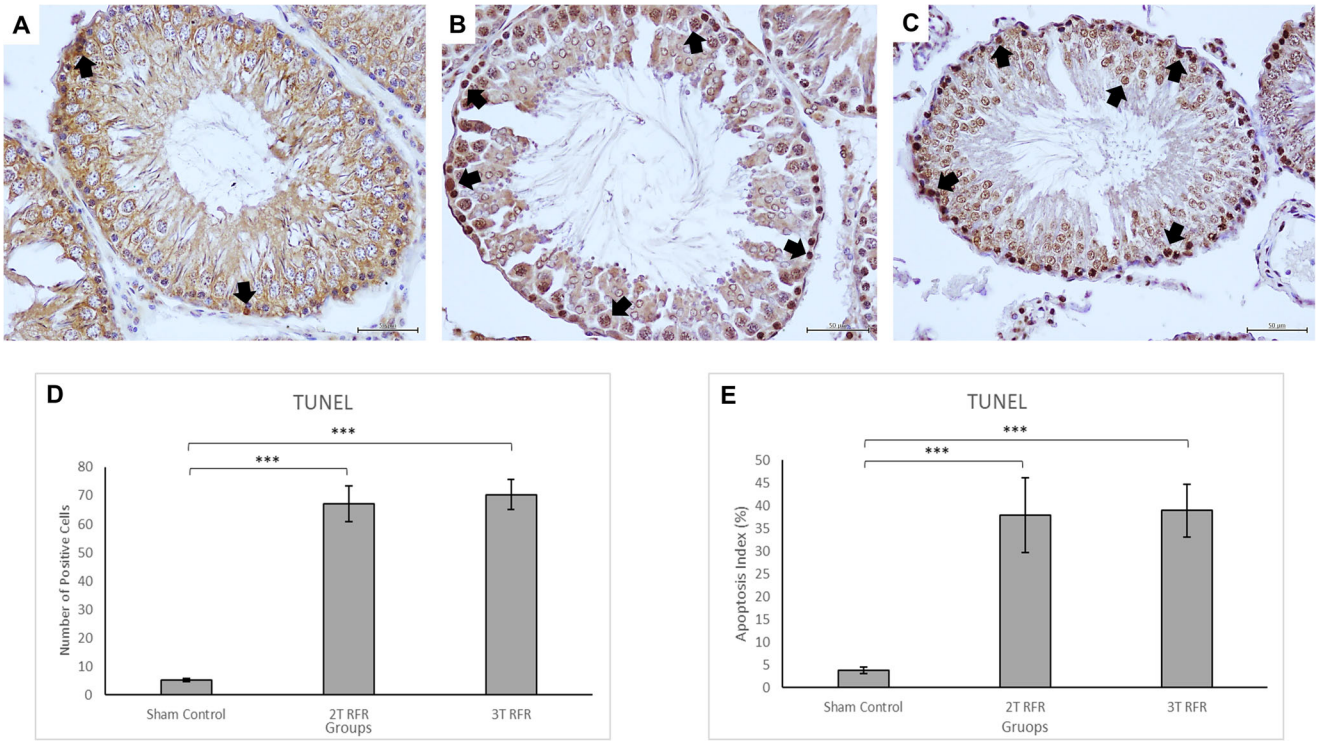


FIGURE 5 | TUNEL staining. Panels A–C show representative TUNEL-stained sections from the sham control (A), 2T RFR (B), and 3T RFR (C) groups. Black arrows indicate TUNEL-positive cells. Panels D and E present bar graphs showing the number of TUNEL-positive cells (D), and apoptosis index (E). The number of TUNEL-positive cells and the apoptosis index increased in the RFR-exposed group, most notably in the 3T RFR group. Data are presented as mean ± SE. Statistical significance: $p < 0.05$ (*), $p < 0.01$ (**), $p < 0.001$ (***), based on Holm–Bonferroni corrected p values. The scale bar is 50 μm.

17496632, 0, Downloaded from https://nyaspubs.onlinelibrary.wiley.com/doi/10.1111/nyas.70116 by Univ of California Lawrence Berkeley National Lab, Wiley Online Library on [11/11/2025]. See the Terms and Conditions (https://onlinelibrary.wiley.com/terms-and-conditions) on Wiley Online Library for rules of use; OA articles are governed by the applicable Creative Commons License

TABLE 1 | Original p values and adjusted p values calculated via Holm–Bonferroni method.

Comparison	Parameter	Raw p value	Adjusted p value
Sham control vs. 3T RFR	Apoptosis index	2.99×10^{-19}	8.77×10^{-18}***
Sham control vs. 3T RFR	TUNEL-positive cells	3.81×10^{-19}	8.77×10^{-18}***
Sham control vs. 2T RFR	Apoptosis index	2.57×10^{-18}	5.66×10^{-17}***
Sham control vs. 2T RFR	TUNEL-positive cells	3.06×10^{-18}	6.42×10^{-17}***
Sham control vs. 3T RFR	γ-H2AX	3.18×10^{-10}	6.36×10^{-9}***
Sham control vs. 3T RFR	SEH	5.11×10^{-9}	9.71×10^{-8}***
2T RFR vs. 3T RFR	SEH	2.78×10^{-8}	5.01×10^{-7}***
2T RFR vs. 3T RFR	Beclin-1	2.65×10^{-7}	4.51×10^{-6}***
Sham control vs. 2T RFR	Johnsen score (JS)	2.85×10^{-5}	4.56×10^{-4}***
Sham control vs. 3T RFR	Beclin-1	5.70×10^{-5}	8.55×10^{-4}***
2T RFR vs. 3T RFR	γ-H2AX	1.47×10^{-4}	2.06×10^{-3}**
2T RFR vs. 3T RFR	STD	1.73×10^{-4}	2.25×10^{-3}**
Sham control vs. 2T RFR	γ-H2AX	0.001	0.012*
Sham control vs. 3T RFR	Johnsen score (JS)	0.0020	0.0220*
Sham control vs. 3T RFR	STD	0.0030	0.0300*
Sham control vs. 3T RFR	Abnormal sperm morphology	0.0040	0.0360*
2T RFR vs. 3T RFR	Johnsen score (JS)	0.0990	0.7920
Sham control vs. 2T RFR	Abnormal sperm morphology	0.1260	0.8820
Sham control vs. 2T RFR	SEH	0.1930	1
Sham control vs. 2T RFR	Beclin-1	0.2930	1
2T RFR vs. 3T RFR	TUNEL-positive cells	0.4060	1
Sham control vs. 2T RFR	STD	0.4250	1
2T RFR vs. 3T RFR	Apoptosis index	0.5460	1
2T RFR vs. 3T RFR	Abnormal sperm morphology	0.6160	1

***$p < 0.001$; **$p < 0.01$; *$p < 0.05$.

A comprehensive account of all comparisons is provided, incorporating both unadjusted p values and p values that have undergone Holm–Bonferroni adjustment. This detailed summary is presented in Table 1.

4 | Discussion

In this study, we investigated whether exposure to 3.5 GHz RFR during the intrauterine period affected the reproductive systems of rats in the first year after birth. To assess long-term effects, we used histological and immunohistochemical techniques, which are highly sensitive in detecting cellular and structural changes. Our findings revealed significant deterioration in testicular histology, abnormal sperm morphology, increased DNA damage, elevated autophagic activity, and activation of apoptotic pathways.

The SAR of 0.0357 W/kg used in this study was intentionally selected to reflect the low-level, chronic RFR exposure commonly encountered in daily life, despite being well below the safety thresholds recommended by international regulatory authorities. Supporting the ecological relevance of our model, previous human studies conducted by our group have reported that a significant proportion of pregnant women use mobile phones for more than 1 h/day and are exposed to RFR associated with Wi-Fi for more than 2 h/day [2, 39–42].

Histological analysis demonstrated significant reductions in seminiferous tubule diameter and epithelial height, accompanied by decreased Johnsen scores in the RFR-exposed groups compared to sham controls. These findings suggest impaired spermatogenesis and testicular atrophy, aligning with previous studies that reported the detrimental effects of RFR exposure on male reproductive health. In a recent study by Yavas et al., the impact of RFR on rat testicular tissue was thoroughly investigated, revealing notable histopathological alterations, including a reduction in the diameter of seminiferous tubules and a decrease in epithelial height. Additionally, an increase in DNA damage within testicular cells was observed, highlighting the potential harmful effects of RFR exposure on testicular integrity [43]. These results are consistent with earlier research suggesting that prolonged or

17496632, 0, Downloaded from https://nyaspubs.onlinelibrary.wiley.com/doi/10.1111/nyas.70116 by Univ of California Lawrence Berkeley National Lab, Wiley Online Library on [11/11/2025]. See the Terms and Conditions (https://onlinelibrary.wiley.com/terms-and-conditions) on Wiley Online Library for rules of use; OA articles are governed by the applicable Creative Commons License

significant RFR exposure may disrupt normal spermatogenesis and contribute to testicular dysfunction. The observed changes in testicular morphology further support the hypothesis that RFR exposure may lead to impaired reproductive function, with the potential for long-term consequences on fertility. Furthermore, Qin et al. investigated the chronotoxicity of RF fields in pubertal testis development. The experimental model comprised 4-week-old mice exposed to RF (1800 MHz, SAR, 0.50 W/kg) in the morning and evening for 3 weeks. Results included pathological changes and functional indices within the testis. Following RF exposure, significant damage was observed in spermatogenesis development, characterized by a smaller seminiferous tubule diameter and a seminiferous epithelium with a reduced number of cells [44].

The increased percentage of abnormal sperm morphology in the RFR-exposed groups suggests that intrauterine RFR exposure disrupts sperm development and maturation processes. To confirm the physiological relevance of our findings, it is important to note that the normal sperm morphology rate observed in our control group (~74%) aligns well with established reference ranges reported in the literature. For instance, van der Horst et al. documented normal sperm morphology ranging from 67% to 74% in healthy rats, while Yılmaz et al. observed approximately 66% normal morphology in control rats [35, 45]. This concordance supports the validity of our control data and underscores that the observed morphological impairments in the exposed groups are likely reflective of true pathological changes rather than methodological artifacts. This alignment with previously reported normative sperm morphology values not only validates our control data but also strengthens the conclusion that the morphological abnormalities observed in RFR-exposed groups are indicative of true pathological effects rather than experimental artifacts. This observation aligns with prior studies highlighting the reproductive toxicity of RFR. For example, Dasdag and Akdag reported that RFR exposure is associated with oxidative stress, a key factor impairing sperm morphology and function [46]. These findings reinforce the hypothesis that RFR can have detrimental effects on male fertility. Additional studies provide substantial evidence supporting this hypothesis. For instance, Özgen et al. demonstrated that Wistar albino rats exposed to 2100 MHz RFR for 90 days exhibited increased abnormal sperm morphology and decreased sperm counts. Notably, these adverse effects were mitigated by melatonin administration, highlighting its potential as a protective intervention [47]. Furthermore, Zhang et al. reported a significant reduction in sperm motility among men, emphasizing that even nonoccupational RFR exposure can adversely affect sperm quality [7]. Collectively, these studies provide compelling evidence that RFR exposure compromises sperm quality, affecting both morphology and function across various species and exposure conditions.

Low-intensity RFR has been increasingly associated with nonthermal biological effects, despite being within international safety limits. Although the exposure intensity in this study was below the ICNIRP safety limits, accumulating evidence supports the existence of nonthermal biological effects caused by low-intensity RFR. Yakymenko et al. reviewed over 100 studies showing that low-level RFR can induce oxidative stress, DNA damage, and cellular dysfunction through nonthermal mechanisms [48]. Similarly, Belpomme et al. emphasized that current safety guidelines focus primarily on thermal effects and do not adequately address these nonthermal health risks, which include neurological disorders, reproductive toxicity, and carcinogenic potential [49]. These findings highlight the importance of investigating subtle, long-term biological effects of low-level RFR exposure, as demonstrated in our study.

Our immunohistochemical analysis revealed elevated expression of γ-H2AX in the RFR-exposed groups, indicating increased DNA damage. Phosphorylation of H2AX known as γ-H2AX has been identified as a biomarker for DNA DSBs. DSBs represent a critical form of genetic damage, with the potential to compromise the integrity of the genome. In response to DNA damage, H2AX is rapidly phosphorylated at serine 139, leading to the formation of γ-H2AX foci at the sites of DSBs. These foci then act as docking sites for repair proteins, thus initiating the DNA repair process [50]. Recent studies have highlighted the significance of γ-H2AX as a biomarker for the assessment of DNA damage. Specifically, γ-H2AX is effective in monitoring the repair of genetic damage and evaluating the response to treatments. Its use is expanding to include the assessment of radiation-induced damage and the monitoring of cancer therapy outcomes [51]. Upregulation of γ-H2AX expression in this study aligns with previous research demonstrating that RFR exposure induces oxidative stress and DNA damage in reproductive tissues, highlighting the genotoxic potential of RFR through oxidative stress-mediated mechanisms. Investigations on DNA breaks and oxidative changes in rat testicular tissue found that high-frequency exposure to 900, 1800, or 2100 MHz RF radiation-induced oxidative stresses [52]. Houston et al. found that exposure of spermatozoa to radiofrequency electromagnetic energy for 5 weeks had a detrimental effect. After 1 week, there was an increase in mitochondrial production of reactive oxygen species (ROS). During all exposure periods, there was an increase in DNA oxidation and degradation [53]. Moreover, Shahin et al. observed significant oxidative stress markers and DNA fragmentation accompanied by lipid peroxidation and histological changes in testicular tissues [54]. Similarly, Akdag et al. found elevated DNA damage in the testes of Wistar albino rats exposed to 2.4 GHz RFR for 24 h daily over 12 months, emphasizing the long-term impact of RFR on reproductive organs [55]. These findings collectively establish a robust link between RFR-induced oxidative stress and DNA damage in reproductive tissues, further validating the elevated γ-H2AX expression observed in this study as a marker of RFR-induced genotoxicity.

Autophagy is a cellular process of "self-eating" degradative activity, in which proteins or entire organelles are broken down in lysosomes and subsequently recycled to satisfy the anabolic and bioenergetic requirements of the cell. This makes them key to tissue homeostasis. Furthermore, various human pathologies, including neurodegeneration, aging, cancer, and autoimmunity, have been associated with deregulated autophagy [56]. We also observed a marked increase in the expression of Beclin-1, particularly in the third-trimester RFR group. Beclin-1, a 60 kDa protein, is located on chromosome 17q21. It has been established that it is a mammalian cell homologue of the yeast autophagy-related gene Atg6, and it has been demonstrated that it mediates the initiation stage of autophagy [57]. Recent studies have shown how oxidative stress, DNA damage, and autophagy are linked. For example, Uribe et al. demonstrated that exposure to ionomycin and hydrogen peroxide induces oxidative stress and activates autophagy

17496632, 0, Downloaded from https://nyaspubs.onlinelibrary.wiley.com/doi/10.1111/nyas.70116 by Univ of California Lawrence Berkeley National Lab, Wiley Online Library on [11/11/2025]. See the Terms and Conditions (https://onlinelibrary.wiley.com/terms-and-conditions) on Wiley Online Library for rules of use; OA articles are governed by the applicable Creative Commons License

in human sperm cells [58]. Moreover, the findings of the study conducted by Hao et al. support the hypothesis that the decrease in miR-30a levels in neurons exposed to microwave radiation positively regulates autophagy by increasing Beclin-1 expression [59]. Similarly, it has been demonstrated that autophagy and DNA damage can be activated through ROS generation induced by radiofrequency EMFs (RF-EMFs). Autophagy has been found to play a protective role in DNA damage caused by RF-EMF exposure. These findings provide evidence for the mechanism by which RF-EMF triggers autophagy and the beneficial role of autophagy in the DNA damage response to RF-EMF exposure [60]. Kumar et al. also reported an increased level of ROS due to microwave exposure. The generation of ROS in the testis is a potential causative agent of toxic effects on the physiology of reproduction [61]. Taken together, these findings indicate that RFR-induced oxidative stress may trigger autophagic pathways in testicular cells. Autophagy may serve as a protective response to mitigate oxidative damage in testicular tissues; however, prolonged or dysregulated autophagy could potentially contribute to cellular dysfunction, raising concerns about the long-term effects of chronic RFR exposure on reproductive health.

The TUNEL assay results revealed a significant increase in apoptotic cells within the testes of RFR-exposed rats, indicating heightened cell death. Apoptosis is a tightly regulated process essential for maintaining testicular homeostasis, as it ensures the elimination of damaged or unnecessary cells. However, excessive apoptosis can disrupt this balance, leading to reduced sperm production and, ultimately, infertility [32, 33]. As previously stated by Xing et al., exposure to 1800 MHz microwave radiation has been shown to induce p53-dependent cell apoptosis through cytochrome c-mediated caspase-3 activation [62]. An increase in free radicals or ROS has been demonstrated to have a detrimental effect on a variety of cellular and physiological processes, including gene expression, calcium release from intracellular storage sites, cell growth, DNA damage and apoptosis. It is therefore hypothesized that the effects of RFR exposure on free radical formation in cells could also affect these cellular functions [63]. Guo et al. reported significant declines in sperm quality following RFR exposure, accompanied by increased apoptosis within testicular cells and alterations in the secretory functions of Sertoli and Leydig cells [64]. These findings collectively support the conclusion that RFR exposure induces apoptosis in testicular cells through oxidative stress and dysregulation of apoptotic signaling pathways, contributing to infertility and impaired reproductive health. Our findings are in agreement with studies reporting increased apoptosis in testicular tissue following RFR exposure.

The mechanisms underlying RFR-induced reproductive toxicity are likely multifaceted, involving oxidative stress, mitochondrial dysfunction, and disruption of key cellular signaling pathways. RFR exposure has been shown to generate ROS, leading to oxidative damage to lipids, proteins, and DNA [63]. Such oxidative stress can compromise cellular integrity and function, particularly in highly sensitive tissues such as the testes. De Iuliis et al. demonstrated that RFR significantly increases ROS production and induces DNA damage in human spermatozoa, highlighting the vulnerability of male germ cells to electromagnetic radiation [65]. The increased DNA damage, autophagy, and apoptosis observed in our study strongly suggest that oxidative stress serves as a central mediator of RFR-induced cellular dysfunction. This cascade of events may not only impair testicular function but also contribute to long-term reproductive toxicity, underscoring the need for further investigation into the molecular pathways linking RFR exposure to male fertility decline.

It is critical to consider the broader implications of these findings for human health. With the increasing prevalence of wireless devices and the corresponding rise in RFR exposure, concerns about its potential impact on male fertility are growing. Although our study was conducted in rats, the results strongly suggest that prenatal RFR exposure could have long-lasting adverse effects on the male reproductive system. Supporting evidence from human studies has demonstrated clear associations between RFR exposure and reduced sperm quality, motility, and viability [16, 65]. In addition, the similarity of birth and adult body weights between the RFR-exposed and control groups suggests that the reproductive impairments observed are not attributable to generalized developmental delays or nutritional deficiencies, further supporting a specific detrimental effect of RFR exposure on the reproductive system. These findings underscore the necessity of implementing precautionary measures to minimize RFR exposure during critical periods, such as pregnancy, and so forth [11]. Such measures may include limiting the use of wireless devices and ensuring adequate protective strategies against electromagnetic radiation.

5 | Conclusion

This study involved monitoring the male offspring of pregnant rats exposed to 3.5 GHz RFR exclusively during the prenatal period, with no exposure to electromagnetic waves for a period of one year following birth. The most original aspect of this study is that young male rats were kept alive for 1 year without any RF radiation exposure except during the prenatal period, and at the end of this period, their reproductive systems were examined. The examinations conducted in the first year after birth showed that exposure to 3.5 GHz RFRs only during the prenatal period poses significant risks to male rat reproductive health. Another original aspect of the study is that the first of the pregnant groups was exposed to RFRs during the three trimesters and the other during the last two trimesters.

Histological changes, increased abnormal sperm morphology, DNA damage, increased autophagic activity, and increased apoptosis are among the observed effects. These findings revealed that the reproductive systems of male offspring exposed to RFRs exclusively during pregnancy were negatively affected, even though they were not exposed to any EMFs for a year after birth, and the observed effects were even more pronounced in the full trimester group. In summary, this study showed that exposure to radiofrequency radiation (RFR) during pregnancy may have a negative impact on the reproductive health of subsequent male generations. Therefore, further molecular and cellular studies are needed to improve our understanding of the relationship between prenatal exposure to 3.5 GHz radiofrequency radiation (RFR) and subsequent male reproductive toxicity, and the mechanisms involved. Future investigations should extend the experimental timeline by incorporating multiple postexposure time points (e.g., 1, 6, and 12 months) to allow for a more comprehensive evaluation of the long-term effects of prenatal RFR exposure on reproductive

17496632, 0, Downloaded from https://nyaspubs.onlinelibrary.wiley.com/doi/10.1111/nyas.70116 by Univ of California Lawrence Berkeley National Lab, Wiley Online Library on [11/11/2025]. See the Terms and Conditions (https://onlinelibrary.wiley.com/terms-and-conditions) on Wiley Online Library for rules of use; OA articles are governed by the applicable Creative Commons License

function. Additionally, detailed assessments of sperm parameters such as motility, as well as organ weights, were not included in the current study. These aspects represent limitations and are planned to be addressed in ongoing and future studies to provide a more comprehensive understanding of the systemic and functional consequences of prenatal RFR exposure. Finally, such research is crucial for developing evidence-based guidelines and implementing precautionary measures to safeguard reproductive health.

Author Contributions

Elif Gelenli Dolanbay: responsible for the overall design of the study methodology, validation, data curation, formal analysis, investigation, resources, writing – original draft. **Tugay Mert**: methodology, investigation, visualization, writing. **Gozde Caliskan Bender**: methodology, investigation, visualization. **Hava Bektas**: methodology, investigation. **Unal Uslu**: methodology, investigation. **Claudio Enrique Fernandez-Rodriguez**: psSAR simulation, methodology. **Suleyman Dasdag**: overall management and guidance of the study, compiling the results for the paper's conclusion.

Acknowledgments

The authors are grateful to Kerem Dolanbay for his consistent support. The authors would like to thank Erkan Erener for his valuable help with the final language editing of the manuscript.

Conflicts of Interest

The authors declare no conflicts of interest.

References

1. A. Yardim, B. Sırav Aral, A. Tomruk, et al., "The Histological and Biochemical Analysis of the Effects of Radiofrequency Radiation on Testis Tissue of Rats and the Protective Effect of Melatonin," *Turkish Journal of Medical Sciences* 54 (2024): 858–865, https://doi.org/10.55730/1300-0144.5857.

2. H. Bektas and S. Dasdag, "Effect of Radiofrequencies Emitted From Mobile Phones and Wi-Fi on Pregnancy," *Journal of International Dental and Medical Research* 10 (2017): 1084–1095.

3. L. Hardell and M. Nilsson, "Summary of Seven Swedish Case Reports on the Microwave Syndrome Associated With 5G Radiofrequency Radiation," *Reviews on Environmental Health* 40 (2024): 147–157, https://doi.org/10.1515/reveh-2024-0017.

4. P. Kaur, U. Rai, and R. Singh, "Genotoxic Risks to Male Reproductive Health From Radiofrequency Radiation," *Cells* 12 (2023): 594, https://doi.org/10.3390/cells12040594.

5. M. Prasad, P. Kathuria, P. Nair, et al., "Mobile Phone Use and Risk of Brain Tumours: A Systematic Review of Association Between Study Quality, Source of Funding, and Research Outcomes," *Neurological Sciences* 38 (2017): 797–810, https://doi.org/10.1007/s10072-017-2850-8.

6. M. Carlberg and L. Hardell, "Evaluation of Mobile Phone and Cordless Phone Use and Glioma Risk Using the Bradford Hill Viewpoints From 1965 on Association or Causation," *BioMed Research International* 2017 (2017): 1–17, https://doi.org/10.1155/2017/9218486.

7. S. Zhang, F. Mo, Y. Chang, et al., "Effects of Mobile Phone Use on Semen Parameters: A Cross-Sectional Study of 1634 Men in China," *Reproduction, Fertility, and Development* 34 (2022): 669–678, https://doi.org/10.1071/RD21234.

8. R. PW Kenny, E. E. Johnson, A. M. Adesanya, et al., "The Effects of Radiofrequency Exposure on Male Fertility: A Systematic Review of Human Observational Studies With Dose–Response Meta-Analysis," *Environment International* 190 (2024): 108817, https://doi.org/10.1016/j.envint.2024.108817.

9. H. Bektas, S. Algul, F. Altindag, et al., "Effects of 3.5 GHz Radiofrequency Radiation on Ghrelin, Nesfatin-1, and Irisin Level in Diabetic and Healthy Brains," *Journal of Chemical Neuroanatomy* 126 (2022): 102168, https://doi.org/10.1016/j.jchemneu.2022.102168.

10. E. Cordelli, L. Ardoino, B. Benassi, et al., "Effects of Radiofrequency Electromagnetic Field (RF-EMF) Exposure on Male Fertility: A Systematic Review of Experimental Studies on Non-Human Mammals and Human Sperm In Vitro," *Environment International* 185 (2024): 108509, https://doi.org/10.1016/j.envint.2024.108509.

11. H. Bektas and S. Dasdag, "The Effects of Radiofrequency Radiation on Male Reproductive Health and Potential Mechanisms," *Electromagnetic Biology and Medicine* 44 (2025): 359–384, https://doi.org/10.1080/15368378.2025.2480664.

12. C. Sage and D. O. Carpenter, eds., *BioInitiative report: A rationale for a biologically-based public exposure standard for electromagnetic fields (ELF and RF)*. (BioInitiative Working Group 2007), https://www.jrseco.com/wp-content/uploads/BioInitiative-2007.pdf.

13. H. Yadav, U. Rai, and R. Singh, "Radiofrequency Radiation: A Possible Threat to Male Fertility," *Reproductive Toxicology* 100 (2021): 90–100, https://doi.org/10.1016/j.reprotox.2021.01.007.

14. R. J. Aitken, L. E. Bennetts, D. Sawyer, et al., "Impact of Radio Frequency Electromagnetic Radiation on DNA Integrity in the Male Germline," *International Journal of Andrology* 28 (2005): 171–179, https://doi.org/10.1111/j.1365-2605.2005.00531.x.

15. S. Dasdag, M. Z. Akdag, E. Ulukaya, et al., "Mobile Phone Exposure Does Not Induce Apoptosis on Spermatogenesis in Rats," *Archives of Medical Research* 39 (2008): 40–44, https://doi.org/10.1016/j.arcmed.2007.06.013.

16. A. Agarwal, N. R. Desai, K. Makker, et al., "Effects of Radiofrequency Electromagnetic Waves (RF-EMW) From Cellular Phones on Human Ejaculated Semen: An In Vitro Pilot Study," *Fertility and Sterility* 92 (2009): 1318–1325, https://doi.org/10.1016/j.fertnstert.2008.08.022.

17. X.-J. Su, W. Yuan, H. Tan, et al., "Correlation Between Exposure to Magnetic Fields and Embryonic Development in the First Trimester," *PLoS ONE* 9 (2014): e101050, https://doi.org/10.1371/journal.pone.0101050.

18. T. Sadeghi, A. Ahmadi, M. Javadian, et al., "Preterm Birth Among Women Living Within 600 Meters of High Voltage Overhead Power Lines: A Case-Control Study," *Romanian Journal of Internal Medicine* 55 (2017): 145–150, https://doi.org/10.1515/rjim-2017-0017.

19. M. Ha, H. Im, M. Lee, et al., "Radio-Frequency Radiation Exposure From AM Radio Transmitters and Childhood Leukemia and Brain Cancer," *American Journal of Epidemiology* 166 (2007): 270–279, https://doi.org/10.1093/aje/kwm083.

20. Z. A. Kashani, R. Pakzad, F. R. Fakari, et al., "Electromagnetic Fields Exposure on Fetal and Childhood Abnormalities: Systematic Review and Meta-analysis," *Open Medicine* 18 (2023): 20230697, https://doi.org/10.1515/med-2023-0697.

21. K. Hug, L. Grize, A. Seidler, et al., "Parental Occupational Exposure to Extremely Low Frequency Magnetic Fields and Childhood Cancer: A German Case-Control Study," *American Journal of Epidemiology* 171 (2010): 27–35, https://doi.org/10.1093/aje/kwp339.

22. E. P. Rogakou, D. R. Pilch, A. H. Orr, et al., "DNA Double-Stranded Breaks Induce Histone H2AX Phosphorylation on Serine 139," *Journal of Biological Chemistry* 273 (1998): 5858–5868, https://doi.org/10.1074/jbc.273.10.5858.

23. A. G. Simon, S. I. Lyu, A. M. Schultheis, et al., "Exploration of Histone Protein γ-H2AX as a Prognostic Factor in Soft Tissue Sarcomas and Its Association With Biological Behavior, Immune Cell Environment and Survival in Leiomyosarcoma," *International Journal of Cancer* 156 (2024): 2237–2250, https://doi.org/10.1002/ijc.35310.

17496632, 0, Downloaded from https://nyaspubs.onlinelibrary.wiley.com/doi/10.1111/nyas.70116 by Univ of California Lawrence Berkeley National Lab, Wiley Online Library on [11/11/2025]. See the Terms and Conditions (https://onlinelibrary.wiley.com/terms-and-conditions) on Wiley Online Library for rules of use; OA articles are governed by the applicable Creative Commons License

24. I. Nishibuchi and S. Tashiro, "DNA Double-Strand Break Repair Capacity and Normal Tissue Toxicity Induced by Radiotherapy," *Journal of Radiation Research* 65 (2024): i52–i56, https://doi.org/10.1093/jrr/rrae081.

25. M. N. Moore, J. I. Allen, and P. J. Somerfield, "Autophagy: Role in Surviving Environmental Stress," *Marine Environment Research* 62 (2006): S420–S425, https://doi.org/10.1016/j.marenvres.2006.04.055.

26. M. Sisakht, M. Darabian, A. Mahmoodzadeh, et al., "The Role of Radiation Induced Oxidative Stress as a Regulator of Radio-adaptive Responses," *International Journal of Radiation Biology* 96 (2020): 561–576, https://doi.org/10.1080/09553002.2020.1721597.

27. D.-P. Jiang, J. Li, J. Zhang, et al., "Long-Term Electromagnetic Pulse Exposure Induces Abeta Deposition and Cognitive Dysfunction Through Oxidative Stress and Overexpression of APP and BACE1," *Brain Research* 1642 (2016): 10–19, https://doi.org/10.1016/j.brainres.2016.02.053.

28. K. Liu, G. Zhang, Z. Wang, et al., "The Protective Effect of Autophagy on Mouse Spermatocyte Derived Cells Exposure to 1800 MHz Radiofrequency Electromagnetic Radiation," *Toxicology Letters* 228 (2014): 216–224, https://doi.org/10.1016/j.toxlet.2014.05.004.

29. N. V. Koshkina, K. Briggs, F. Palalon, et al., "Autophagy and Enhanced Chemosensitivity in Experimental Pancreatic Cancers Induced by Non-invasive Radiofrequency Field Treatment," *Cancer* 120 (2014): 480–491, https://doi.org/10.1002/cncr.28453.

30. Y. H. Hao, L. Zhao, and R. Y. Peng, "Effects of Electromagnetic Radiation on Autophagy and Its Regulation," *Biomedical and Environmental Sciences* 31 (2018): 57–65, https://doi.org/10.3967/bes2018.006.

31. R. Kang, H. J. Zeh, M. T. Lotze, et al., "The Beclin 1 Network Regulates Autophagy and Apoptosis," *Cell Death and Differentiation* 18 (2011): 571–580, https://doi.org/10.1038/cdd.2010.191.

32. K. Kyrylkova, S. Kyryachenko, M. Leid, and C. Kioussi, "Detection of Apoptosis by TUNEL Assay," in *Odontogenesis: Methods in Molecular Biology*, ed. C. Kioussi vol. 887 (Humana Press 2012), https://doi.org/10.1007/978-1-61779-860-3_5.

33. M. Saygin, S. Caliskan, N. Karahan, et al., "Testicular Apoptosis and Histopathological Changes Induced by a 2.45 GHz Electromagnetic Field," *Toxicology and Industrial Health* 27 (2011): 455–463, https://doi.org/10.1177/0748233710389851.

34. A. E. Alsemeh, M. M. Ahmed, and A. Fawzy, "Vitamin E Rescues Valproic Acid-Induced Testicular Injury in Rats: Role of Autophagy," *Life Sciences* 296 (2022): 120434, https://doi.org/10.1016/j.lfs.2022.120434.

35. G. Yılmaz, Ü. Eren, Ö. Güleş, et al., "Investigation of the Effects of Selenium Against 4-Nonylphenol-Induced Toxicity in Rat Testis," *Biological Trace Element Research* 203 (2025): 4774–4788, https://doi.org/10.1007/s12011-025-04539-8.

36. L.-W. Xie, S. Cai, H.-Y. Lu, et al., "Microbiota-Derived I3A Protects the Intestine Against Radiation Injury by Activating AhR/IL-10/Wnt Signaling and Enhancing the Abundance of Probiotics," *Gut Microbes* 16 (2024): 2347722, https://doi.org/10.1080/19490976.2024.2347722.

37. Y. Kucukbagriacik, M. Dastouri, E. Ozgur-Buyukatalay, et al., "Investigation of Oxidative Damage, Antioxidant Balance, DNA Repair Genes, and Apoptosis due to Radiofrequency-Induced Adaptive Response in Mice," *Electromagnetic Biology and Medicine* 41 (2022): 389–401, https://doi.org/10.1080/15368378.2022.2117187.

38. W. J. Conover, *Practical_Nonparametric_Statistics*, 2nd ed. (Wiley, 1980).

39. H. Bektas, M. S. Bektas, and S. Dasdag, "Effects of Mobile Phone Exposure on Biochemical Parameters of Cord Blood: A Preliminary Study," *Electromagnetic Biology and Medicine* 37 (2018): 184–191, https://doi.org/10.1080/15368378.2018.1499033.

40. H. Bektas, S. Dasdag, and M. S. Bektas, "Comparison of Effects of 2.4 GHz Wi-Fi and Mobile Phone Exposure on human Placenta and Cord Blood," *Biotechnology & Biotechnological Equipment* 34 (2020): 154–162, https://doi.org/10.1080/13102818.2020.1725639.

41. H. Bektaş, S. Daşdağ, and M. S. Bektaş, "Does Mobile Phone Use of Women During Pregnancy Cause Hearing Problems in Infants? Preliminary Observation," *Perinatal Journal* 28 (2020): 101–107, https://doi.org/10.2399/prn.20.0282013.

42. H. Bektas, M. S. Bektas, and S. Dasdag, "Effect of Mobile Phone Usage Duration During Pregnancy on the General Motor Movements of Infants," *Biotechnology & Biotechnological Equipment* 36 (2022): 57–67, https://doi.org/10.1080/13102818.2022.2046505.

43. M. C. Yavas, A. Kilitci, E. Çelik, et al., "Rat Brain and Testicular Tissue Effects of Radiofrequency Radiation Exposure: Histopathological, DNA Damage of Brain and qRT-PCR Analysis," *International Journal of Radiation Research* 22 (2024): 529–536, https://doi.org/10.61186/ijrr.22.3.529.

44. F. Qin, H. Cao, C. Feng, et al., "Microarray Profiling of LncRNA Expression in the Testis of Pubertal Mice Following Morning and Evening Exposure to 1800 MHz Radiofrequency Fields," *Chronobiology International* 38 (2021): 1745–1760, https://doi.org/10.1080/07420528.2021.1962902.

45. G. van der Horst, B. Skosana, A. Legendre, et al., "Cut-Off Values for Normal Sperm Morphology and Toxicology for Automated Analysis of Rat Sperm Morphology and Morphometry," *Biotechnic & Histochemistry* 93, no. 1 (2018): 49–58, https://doi.org/10.1080/10520295.2017.1380842.

46. S. Dasdag and M. Z. Akdag, "The Link Between Radiofrequencies Emitted From Wireless Technologies and Oxidative Stress," *Journal of Chemical Neuroanatomy* 75 (2016): 85–93, https://doi.org/10.1016/j.jchemneu.2015.09.001.

47. M. Özgen, G. Take, İ. Kaplanoğlu, et al., "Therapeutic Effects of Melatonin in Long-Term Exposure to 2100 MHz Radiofrequency Radiation on Rat Sperm Characteristics," *Revista Internacional de Andrología* 21 (2023): 100371, https://doi.org/10.1016/j.androl.2023.100371.

48. I. Yakymenko, O. Tsybulin, E. Sidorik, et al., "Oxidative Mechanisms of Biological Activity of Low-Intensity Radiofrequency Radiation," *Electromagnetic Biology and Medicine* 35 (2016): 186–202, https://doi.org/10.3109/15368378.2015.1043557.

49. D. Belpomme, L. Hardell, I. Belyaev, et al., "Thermal and Non-Thermal Health Effects of Low Intensity Non-Ionizing Radiation: An International Perspective," *Environmental Pollution* 242 (2018): 643–658, https://doi.org/10.1016/j.envpol.2018.07.019.

50. A. Kinner, W. Wu, C. Staudt, et al., "H2AX in Recognition and Signaling of DNA Double-Strand Breaks in the Context of Chromatin," *Nucleic Acids Research* 36 (2008): 5678–5694, https://doi.org/10.1093/nar/gkn550.

51. U.-S. Lee, D.-H. Lee, and E.-H. Kim, "Characterization of γ-H2AX Foci Formation Under Alpha Particle and X-Ray Exposures for Dose Estimation," *Scientific Reports* 12 (2022): 3761, https://doi.org/10.1038/s41598-022-07653-y.

52. I. Hasan, T. Amin, M. D. R. Alam, et al., "Hematobiochemical and Histopathological Alterations of Kidney and Testis due to Exposure of 4G Cell Phone Radiation in Mice," *Saudi Journal of Biological Sciences* 28 (2021): 2933–2942, https://doi.org/10.1016/j.sjbs.2021.02.028.

53. B. J. Houston, B. Nixon, K. E. McEwan, et al., "Whole-Body Exposures to Radiofrequency-Electromagnetic Energy Can Cause DNA Damage in Mouse Spermatozoa via an Oxidative Mechanism," *Scientific Reports* 9 (2019): 17478, https://doi.org/10.1038/s41598-019-53983-9.

54. N. N. Shahin, N. A. El-Nabarawy, A. S. Gouda, et al., "The Protective Role of Spermine Against Male Reproductive Aberrations Induced by Exposure to Electromagnetic Field – An Experimental Investigation in the Rat," *Toxicology and Applied Pharmacology* 370 (2019): 117–130, https://doi.org/10.1016/j.taap.2019.03.009.

55. M. Z. Akdag, S. Dasdag, F. Canturk, et al., "Does Prolonged Radiofrequency Radiation Emitted From Wi-Fi Devices Induce DNA Damage in Various Tissues of Rats?," *Journal of Chemical Neuroanatomy* 75 (2016): 116–122, https://doi.org/10.1016/j.jchemneu.2016.01.003.

17496632, 0, Downloaded from https://nyaspubs.onlinelibrary.wiley.com/doi/10.1111/nyas.70116 by Univ of California Lawrence Berkeley National Lab, Wiley Online Library on [11/11/2025]. See the Terms and Conditions (https://onlinelibrary.wiley.com/terms-and-conditions) on Wiley Online Library for rules of use; OA articles are governed by the applicable Creative Commons License

56. N. Mizushima, B. Levine, A. M. Cuervo, et al., "Autophagy Fights Disease Through Cellular Self-Digestion," *Nature* 451 (2008): 1069–1075, https://doi.org/10.1038/nature06639.

57. X. H. Liang, L. K. Kleeman, H. H. Jiang, et al., "Protection Against Fatal Sindbis Virus Encephalitis by Beclin, a Novel Bcl-2-Interacting Protein," *Journal of Virology* 72 (1998): 8586–8596, https://doi.org/10.1128/JVI.72.11.8586-8596.1998.

58. P. Uribe, J. Meriño, C. E. Matus, et al., "Autophagy Is Activated in Human Spermatozoa Subjected to Oxidative Stress and Its Inhibition Impairs Sperm Quality and Promotes Cell Death," *Human Reproduction* 37 (2022): 680–695, https://doi.org/10.1093/humrep/deac021.

59. Y. Hao, W. Li, H. Wang, et al., "Microwave Radiation Induces Neuronal Autophagy Through miR-30a-5p/AMPKα2 Signal Pathway," *Bioscience Reports* 42 (2022): BSR20212584, https://doi.org/10.1042/BSR20212584.

60. R. Li, M. Ma, L. Li, et al., "The Protective Effect of Autophagy on DNA Damage in Mouse Spermatocyte-Derived Cells Exposed to 1800 MHz Radiofrequency Electromagnetic Fields," *Cellular Physiology and Biochemistry* 48 (2018): 29–41, https://doi.org/10.1159/000491660.

61. S. Kumar, K. K. Kesari, and J. Behari, "Influence of Microwave Exposure on Fertility of Male Rats," *Fertility and Sterility* 95 (2011): 1500–1502, https://doi.org/10.1016/j.fertnstert.2010.04.078.

62. F. Xing, Q. Zhan, Y. He, et al., "1800 MHz Microwave Induces p53 and p53-Mediated Caspase-3 Activation Leading to Cell Apoptosis In Vitro," *PLoS ONE* 11 (2016): e0163935, https://doi.org/10.1371/journal.pone.0163935.

63. K. K. Kesari, S. Kumar, J. Nirala, et al., "Biophysical Evaluation of Radiofrequency Electromagnetic Field Effects on Male Reproductive Pattern," *Cell Biochemistry and Biophysics* 65 (2013): 85–96, https://doi.org/10.1007/s12013-012-9414-6.

64. L. Guo, J.-J. Lin, Y.-Z. Xue, et al., "Effects of 220 MHz Pulsed Modulated Radiofrequency Field on the Sperm Quality in Rats," *International Journal of Environmental Research and Public Health* 16 (2019): 1286, https://doi.org/10.3390/ijerph16071286.

65. G. N. De Iuliis, R. J. Newey, B. V. King, et al., "Mobile Phone Radiation Induces Reactive Oxygen Species Production and DNA Damage in Human Spermatozoa In Vitro," *PLoS ONE* 4 (2009): e6446, https://doi.org/10.1371/journal.pone.0006446.

17496632, 0, Downloaded from https://nyaspubs.onlinelibrary.wiley.com/doi/10.1111/nyas.70116 by Univ of California Lawrence Berkeley National Lab, Wiley Online Library on [11/11/2025]. See the Terms and Conditions (https://onlinelibrary.wiley.com/terms-and-conditions) on Wiley Online Library for rules of use; OA articles are governed by the applicable Creative Commons License